Geological Magazine

A Tonian age for the Visingsö Group in Sweden constrained by detrital zircon dating and biochronology: implications for evolutionary events

Małgorzata Moczydłowska, Victoria Pease, Sebastian Willman, Linda Wickström & Heda Agić

Online Supplementary Material

Appendix S1. Details of analytical methods

Analytical methods follow those described in Zhang *et al.* (2015*a,b*). Zircons were analyzed for U, Th and Pb isotopes using an ESI NWR-193 excimer laser coupled to a Thermo XSeries2 quadrupole ICP-MS at the PetroTectonics Analytical Facility, Department of Geological Sciences, Stockholm University. Analytical conditions and parameters are summarized in Table S1. Each analysis consisted of 30 seconds background acquisition followed by 40 seconds of data acquisition and 15 seconds wash-out using a 25 µm spot size. He was used as the ablation carrier gas to minimize sample redeposition from the aerosol and stabilize signal intensities (Eggins *et al*. 1998; Günther & Heinrich, 1999; Horn *et al.* 2001). The instrument was tuned for maximum sensitivity of Pb and U while keeping ThO/Th below 0.5 %. The tubing from the ablation chamber to the ICP source was equipped with a signal smoothing device consisting of several Tygon® tubes to split the stream and recombine it. External standardization was performed using Plešovice zircon (Sláma *et al*. 2008), analyzed at the start and end of the analytical sequence and bracketing a maximum of 10 analyses by two measurements of standard zircon. Zircon FC-5z from the Duluth Gabbro (Paces & Miller Jr, 1993) was treated as a known-unknown to control data accuracy.

Table S1. Analytical conditions and parameters

Laser ablation:	
Laser excimer	ESI New Wave ArF 193 nm
Energy density	7 J cm^{-2}
Frequency	10 Hz
Beam diameter	25 µm
ICP-MS:	
Instrument	Thermo XSeries2 quadrupole
Plasma power [W]	1400
Sample gas [l/min]	500
Auxiliary gas [l/min]	0.72
Cooling gas [l/min]	13
Nebulizer gas [l/min]	0.94
Acquisition mode counting	pulse
Dwell times (ms)	^{200}Hg (20), ^{201}Hg (20), ^{202}Hg (40), ^{204}Pb (50), ^{206}Pb (50), ^{207}Pb (50), ^{208}Pb (50), ^{232}Th (40), ^{235}U (50), ^{238}U (50), ^{248}ThO (20)
Standards:	
External	Plesovice (Slama et al., 2008)
Secondary	FC-5z (Paces and Miller, Jr., 1993)

Data reduction and calculation of ratios and ages were performed off-line using the software Iolite (Hellstrom *et al*. 2008; Paton *et al.* 2011) and the VizualAge data reduction scheme of Petrus and Kamber (2012). The down-hole isotopic fractionation correction follows Paton *et al*. (2011) and common Pb is monitored on mass 204 (^{204}Pb + ^{204}Hg).

Analytical results are presented in Table S2, and Figures S1, S2, and S3. Errors are reported at the 2-sigma level. For zircon ages younger than 1.2 Ga the ^{206}Pb/^{238}U ages were used for the final analysis and for ages older than 1.2 Ga the ^{207}Pb/^{206}Pb ages were selected for the final analysis. Analyses with high common Pb as well as those with >10% discordance or >10% uncertainties, were excluded from the final data synthesis. Concordia diagrams and probability density distribution plots were made using ISOPLOT/Ex 4.15 (Ludwig, 2008) (Figs. S1, S2, S3). Excluded analyses are marked by an asterisk in online Supplementary Material Table S2 (U–Pb data Excel file) available at http://journals.cambridge.org/geo.

Provenance of the Visingsö Group. The provenance of the Visingsö zircons is consistent with derivation from the Sveconorwegian orogenic belt and sources within it. These include igneous, metamorphic and recycled sedimentary rocks exposed in the region at the time of deposition, i.e. Svecokarelian rocks (c. 2.0–1.75 Ga), TIB (c. 1.86–1.66 Ga plutonic and volcanic rocks), and metamorphic and igneous rocks associated with the Gothian (1.66–1.52 Ga), Hallandian (c. 1.47–1.38 Ga), and Sveconorwegian (c. 1.14–0.90 Ga) orogens (Lundmark and Lamminen, 2016; Möller *et al*. 2015). Swarms of 1.6–0.95 Ga dolerite dikes also intrude Fennoscandian basement (Söderlund *et al*. 2005).

Meso- to Neoproterozoic sediments now only locally preserved across the shield are also potential sources (Fig. 1A). These 'Jotnian' sandstones, broadly 1.6–0.9 Ga in age, are red continental siliciclastic rocks associated with local marine ingressions (Morad & Al-Aasm, 1994) and include the Almesåkra Group and the Dala Sandstone Formation in Sweden, the Trysil sandstone in Norway, and the Muhos and Hailuoto formations in Finland (see Bingen *et al.* 2011; Lundmark & Lamminen, 2016). The Dala Sandstone Formation has a maximum age of 1.59–1.58 Ga with prominent zircon peaks between c. 1.61–1.88 Ga (Lundmark & Lamminen, 2016). The sandstones and schists of the allochthonous Sparagmite basins in the Caledonides have zircon ages that range from 1990–860 Ma with peaks at 1645, 1600, 1490, 1280, 1155, 965, and 930 Ma, are inferred to have been mostly derived locally – this includes sources within the Sveconorwegian belt that may include a far-traveled Laurentian component, as well as sources from east of the belt in Fennoscandia (Bingen *et al*. 2011).

Similar sources are recognized for the first time in the Visingsö Group, though the provenance of its lower formation is distinct from its middle formation. The lower formation sample V15-Lem is dominated by late Mesoproterozoic to early Neoproterozoic peaks at c. 1026, 945, and 900 Ma, with lesser peaks at c. 1600, 1446, 1268 and 1100 Ma. The middle formation sample V15-9 is dominated by Mesoproterozoic zircon (age peaks at c. 1640, 1580, and 1439 Ma), while older (c. 1780 Ma) and younger ages (c. 1260–1045 Ma) are lesser contributors. Sample V15-10 is dominated by Palaeoproterozoic to Mesoproterozoic zircon, with age peaks at c. 1751, 1625, and 1450 Ma, a spread of ages at c. 1300–990 Ma, and a minor peak at c. 992 Ma. The notable dominance of Sveconorwegian-aged detritus in the lower formation dramatically decreases up-section where Hallandian, Gothian, and Svecokarelian sources dominate. This suggests a changing source region/drainage pattern for these sediments, likely due to burial or re-routing of Sveconorwegian sources. Sediment provenance is generally consistent with local derivation, however sources for the small (8–14%) c. 1.2–1.3 Ga component require voluminous and persistent northwards transport across the Panthalassa margin of Rodinia (e.g. Bingen *et al*. 2011). This is also in agreement with combined sediment provenance and paleocurrent data from clastic rocks of Finnmark, which indicate sources from the south (Zhang *et al*. 2015a, b).

References.

BINGEN, B., BELOUSOVA, E. A. & GRIFFIN, W. L. 2011. Neoproterozoic recycling of the Sveconorwegian orogenic belt: Detrital-zircon data from the Sparagmite basins in the Sveconorwegian Caledonides. *Precambrian Research* **189**, 347–367.

EGGINS, S., KINSLEY, L. & SHELLEY, J. 1998. Deposition and element fractionation processes during atmospheric pressure laser sampling for analysis by ICP-MS. *Applied Surface Science* **127**, 278–286, doi: 10.1016/S0169-4332 (97)00643-0.

GÜNTHER, D., & HEINRICH, C. A. 1999. Enhanced sensitivity in laser ablation-ICP mass spectrometry using helium-argon mixtures as aerosol carrier. *Journal of Analytical Atomic Spectrometry* **14**, 1363–1368, doi: 10.1039 /a901648a.

HELLSTROM, J., PATON, C., WOODHEAD, J. & HERGT, J. 2008. Iolite: Software for spatially resolved LA-(quad and MC) ICPMS analysis. *Mineralogical Association of Canada Short Course* **40**, 343–348.

HORN, I., GUILLONG, M. & GÜNTHER, D. 2001. Wavelength dependent ablation rates for metals and silicate glasses using homogenized laser beam profiles—Implications for LA-ICP-MS: Applied Surface Science, v. 182, p. 91–102, doi: 10.1016 /S0169-4332 (01)00465-2.Ludwig, K.R., 2008, Users' Manual for Isoplot 3.70. *A Geochronological Toolkit for Microsoft Excel: Berkeley Geochronology Center Special Publication*, 4, 1–77.

LUNDMARK, A. M. & LAMMINEN, J. 2016. The provenance and setting of the Mesoproterozoic Dala Sandstone, western Sweden, and paleogeographic implications for southwestern Fennoscandia. *Precambrian Research* **275**, 197–208.

MORAD, S., & AL-AASM, I.S., 1994, Conditions of formation and diagenetic evolution of Upper Proterozoic phosphate nodules from southern Sweden: evidence from petrology, mineral chemistry and isotopes. *Sedimentary Geology* **88**, 267–282.

MÖLLER, C., ANDERSSON, J., DYCK, B. & LUNDIN, I. 2015. Exhumation of an eclogite terrane as a hot migmatitic nappe, Sveconorwegian orogeny. *Lithos* **226**, 147–168.

PACES, J. B. & MILLER, J.D., Jr. 1993. Precise U-Pb ages of Duluth complex and related mafic intrusions, northeastern Minnesota: Geochronological insights to physical, petrogenetic, paleomagnetic, and tectonomagmatic processes associated with the 1.1 Ga Midcontinent Rift system. *Journal of Geophysical Research* **98 (B8**), 13997–14013, doi: 10 .1029 /93JB01159.

PATON, C., HELLSTROM, J., PAUL, B., WOODHEAD, J. & HERGT, J. 2011. Iolite: Freeware for the visualisation and processing of mass spectrometric data. *Journal of Analytical Atomic Spectrometry* **26**, 2508–2518, doi: 10 .1039 /c1ja10172b.

PETRUS, J. A. & KAMBER, B. S. 2012. VizualAge: A novel approach to laser ablation ICP-MS U-Pb geochronology data reduction. *Geostandards and Geoanalytical Research* **36 (3)**, doi: 10.1111 /j .1751-908X .2012 .00158.x.

SLÁMA, J., KOSLER, J., CONDON, D. J., CROWLEY, J. L., GERDES, A., HANCHAR, J. M., HORSTWOOD, M. S. A., MORRIS, G. A., NASDALA, L., NORBERG, N., SCHALTEGGER, U., SCHOENE, B., TUBRETT, M. N. & WHITEHOUSE, M. J. 2008. Plesovice zircon-A new natural reference material for U-Pb and Hf isotopic microanalysis: *Chemical Geology* **249**, 1–35, doi: 10.1016 /j chemgeo.2007.11.005.

SÖDERLUND, U., ISACHSEN, C., BYLUND, G., HEAMAN, L. M., PATCHETT, P. J., VERVOORT, J. & ANDERSSON, U.B. 2005, U-Pb baddeleyite ages and Hf, Nd isotope chemistry constraining repeated mafic magmatism in the Fennoscandian Shield from 1.6 to 0.9 Ga. *Contributions to Mineralogy and Petrology* **150**, 174-194.

ZHANG, W., ROBERTS, D. & PEASE, V. 2015*a*, Provenance characteristics and regional implications of Neoproterozoic, Timanian-margin successions and a basal Caledonian nappe in northern Norway. *Precambrian Research* **268**, 153–167.

ZHANG, W., ROBERTS, D. & PEASE, V. 2015*b*, Provenance of sandstones from Caledonian nappes in Finnmark, Norway: Implications for Neoproterozoic–Cambrian palaeogeography. *Tectonophysics*, http://dx.doi.org/10.1016/j.tecto.2015.09.001.
ZHANG, X., PEASE, V., SKOGSEID, J. & WOHLGEMUTH-UEBERWASSER, C. 2015. Reconstruction of tectonic events on the northern Eurasia margin of the Arctic, from U-Pb detrital zircon provenance investigations of late Paleozoic to Mesozoic sandstones in southern Taimyr Peninsula. *Geological Society of America Bulletin* **128**, 29-46, doi:10.1130/B31241.1.

APPENDIX S2. List of species of organic-walled microfossils in the Visingsö Group

Eukaryotic unicellular taxa:

Cerebrosphaera globosa (Ogurtsova and Sergeev, 1989) Sergeev and Schopf, 2010
Chuaria circularis (Walcott, 1899) Vidal and Ford, 1985
Germinosphaera bispinosa (Mikhailova, 1986) Butterfield, 1994
Lanulatisphaera laufeldii (Vidal, 1976) Porter and Riedman, 2016
Leiosphaeridia ternata (Timofeev, 1966) Mikhailova and Jankauskas, 1989
Leiosphaeridia div.sp.
Macroptycha uniplicata Timofeev, 1976
Navifusa majensis Pyatiletov, 1980
Octoedryxium truncatum Rydavskaya, 1973
Pterospermopsimorpha insolita (Timofeev, 1969) Mikhailova, 1989
Pterospermopsimorpha pileiformis (Timofeev, 1969) Mikhailova, 1989
Schizofusa sp.
Simia annulare (Timofeev, 1969) Mikhailova, 1989
Simia simica (Jankauskas, 1980) Jankuskas, 1989
Squamosphaera colonialica (Jankauskas, 1979) Tang et al., 2015
Tasmanites sp.
Valeria lophostriata (Jankauskas, 1979) Jankauskas, 1982
Vandalosphaeridium reticulatum (Vidal, 1976) Vidal, 1981

Eukaryotic multicellular taxa

Ostiana microcystis Hermann, 1976
Synsphaeridium sp.

Cyanobacterial taxa

Eoschizothryx composita Seng-Joo and Golubic, 1998
Eosynechococcus moorei Hofmann, 1976
Oscillatoriopsis sp.
Palaeolyngbya catenata Hermann, 1974
Polythrichoides lineatus (Hermann, 1974) Hofmann, 1976
Sphaerocongregus variabilis Moorman, 1974
Siphonophycus div.sp.

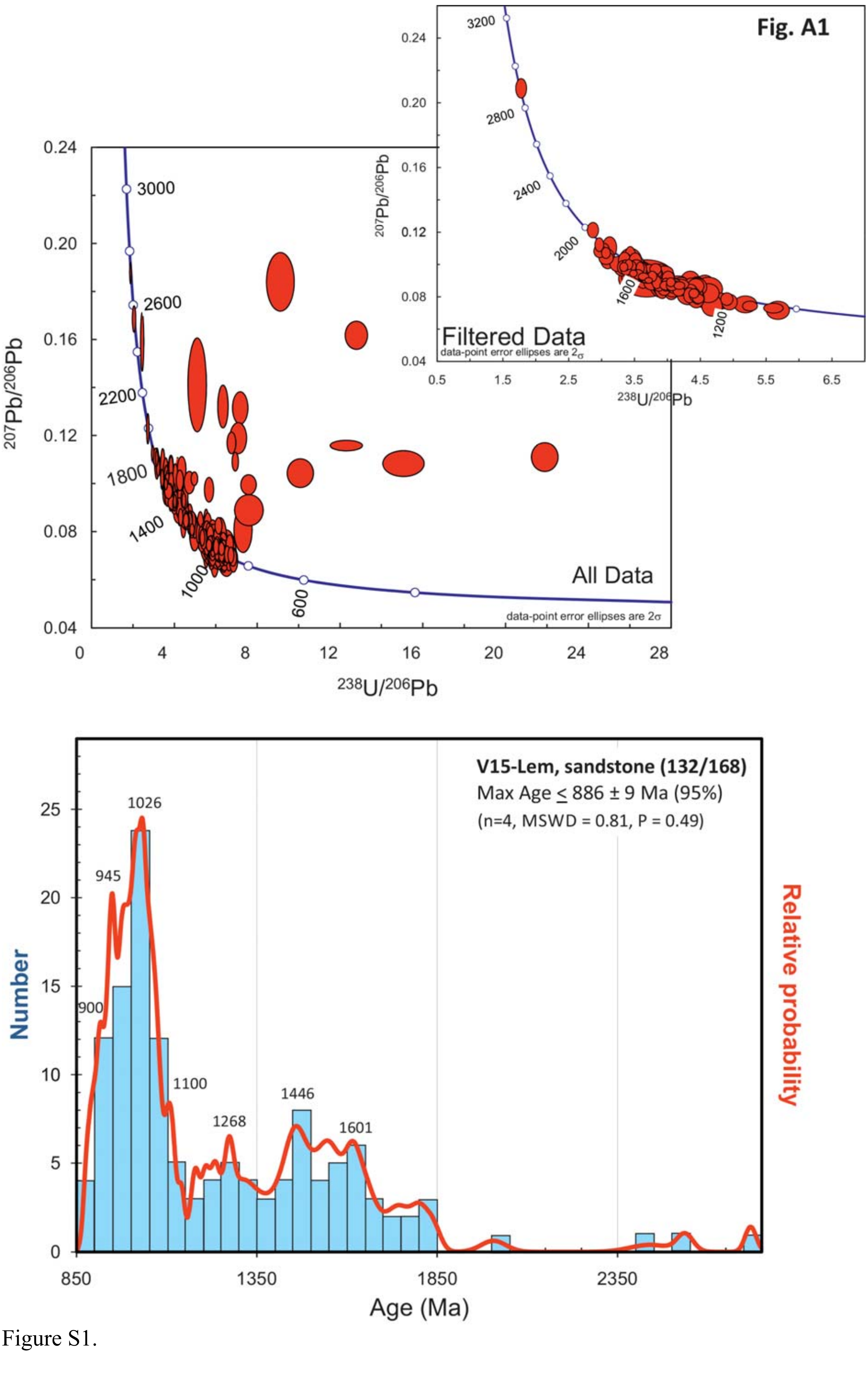

Fig. A1
Filtered Data
data-point error ellipses are 2σ
3200
2800
2400
2000
1600
1200
0.24
0.20
0.16
0.12
0.08
0.04
0.5
1.5
2.5
3.5
4.5
5.5
6.5
207Pb/206Pb
238U/206Pb
All Data
data-point error ellipses are 2σ
3000
2600
2200
1800
1400
1000
600
0
4
8
12
16
20
24
28
V15-Lem, sandstone (132/168)
Max Age ≤ 886 ± 9 Ma (95%)
(n=4, MSWD = 0.81, P = 0.49)
1026
945
900
1100
1268
1446
1601
Number
Relative probability
0
5
10
15
20
25
850
1350
1850
2350
Age (Ma)

Figure S1.

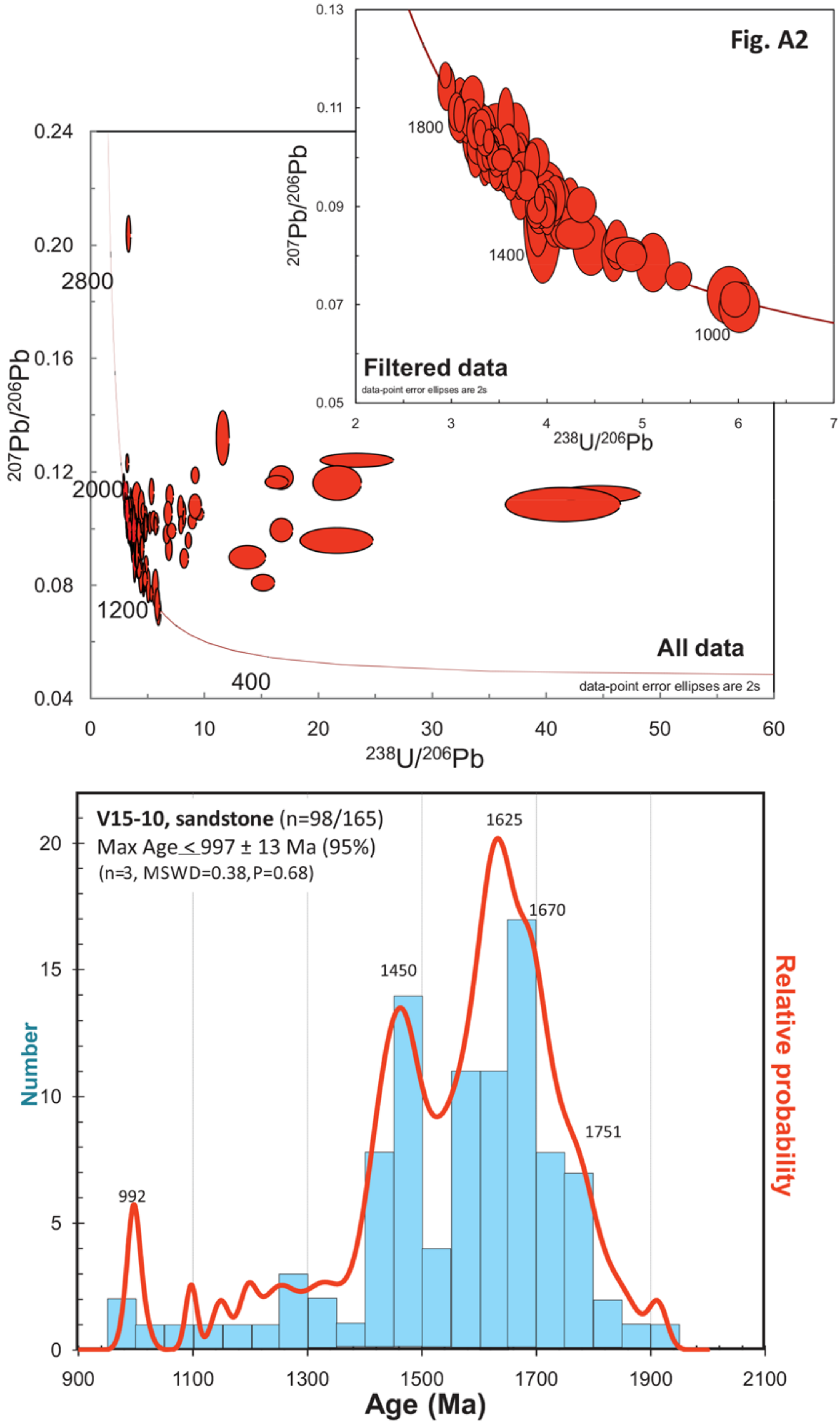
Fig. A2
Filtered data
data-point error ellipses are 2s
1800
1400
1000
$^{207}Pb/^{206}Pb$
$^{238}U/^{206}Pb$
All data
data-point error ellipses are 2s
2800
2000
1200
400
$^{207}Pb/^{206}Pb$
$^{238}U/^{206}Pb$
V15-10, sandstone (n=98/165)
Max Age ≤ 997 ± 13 Ma (95%)
(n=3, MSWD=0.38, P=0.68)
992
1450
1625
1670
1751
Number
Relative probability
Age (Ma)

Figure S2.

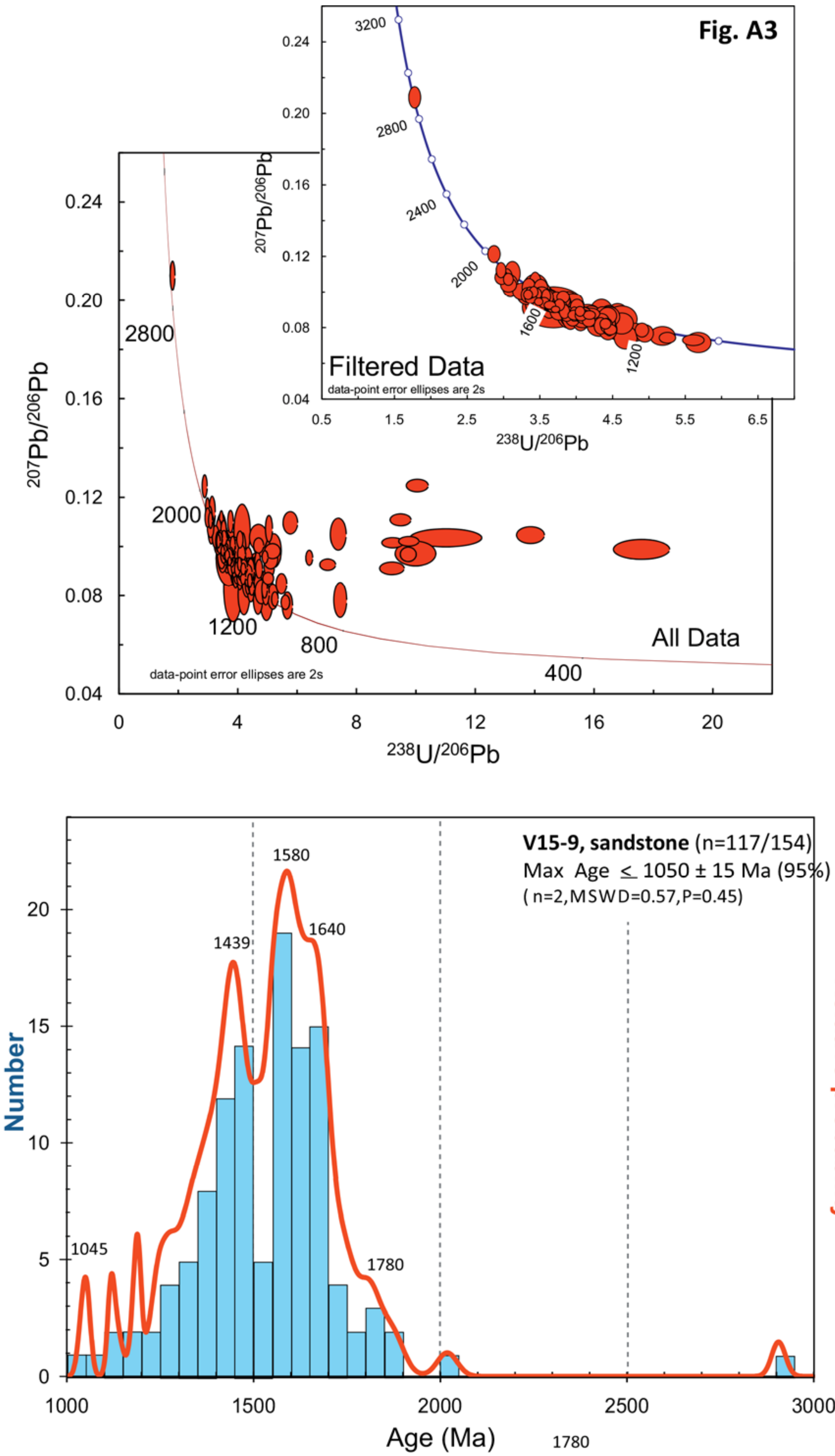
Fig. A3
Filtered Data
data-point error ellipses are 2s
3200
2800
2400
2000
1600
1200
0.24
0.20
0.16
0.12
0.08
0.04
0.5
1.5
2.5
3.5
4.5
5.5
6.5
$^{207}Pb/^{206}Pb$
$^{238}U/^{206}Pb$
All Data
data-point error ellipses are 2s
2800
2000
1200
800
400
0
4
8
12
16
20
V15-9, sandstone (n=117/154)
Max Age ≤ 1050 ± 15 Ma (95%)
(n=2, MSWD=0.57, P=0.45)
1580
1439
1640
1045
1780
Number
Relative probability
0
5
10
15
20
1000
1500
2000
2500
3000
Age (Ma)
1780

Figure S3.